PHYSICAL REVIEW B VOLUME 30, NUMBER 10 15 NOVEMBER 1984

"Folded" optical phonons in $GaAs/Ga_{1-x}Al_xAs$ superlattices

Bernard Jusserand and Daniel Paquet
Laboratoire de Bagneux, Centre National d' Études des Télécommunications, 196 rue de Paris, 92220 Bagneux, France

André Regreny
Centre National d' Études des Télécommunications, Division ICM, Route de Trégastel, Boîte Postale, 40, 22301 Lannion, France

(Received 23 July 1984)

We report the first experimental study, by means of Raman scattering, of "folded" longitudinal optical (LO) phonons in $GaAs/Ga_{1-x}Al_xAs$ superlattices. We successfully analyze their frequency shift and Raman activity in terms of a Kronig-Penney model of lattice dynamics. The LO phonons are either localized in the GaAs "well" or propagating in both layers.

In this paper, we present the first study, both experimental and theoretical, of folded optical phonons in $GaAs/Ga_{1-x}Al_xAs$ superlattices. As it is well known, the new periodicity in the growth direction induces a folding of the Brillouin zone, which implies the onset in the zone center of new phonon modes, possibly Raman active. Many studies have been already devoted to the acoustical vibrations in these new structures.[1-3] The outstanding result is that the acoustical phonons propagate in both materials, unlike, for example, the electrons, which are mostly confined in one of the materials. Concerning the optical phonons, we have reported recently[4] the first unambiguous observation of a "folded" longitudinal optical (LO) line in a $GaAs/Ga_{0.7}Al_{0.3}As$ superlattice. In this paper we present and carefully analyze similar results obtained on several samples: we observed up to the third folded line. The outstanding conclusion of our work is that the "folded optical phonons" in $GaAs/Ga_{1-x}Al_xAs$ superlattices are either localized, weakly localized, or propagative, highly depending on their frequency.

The studied samples have been grown by molecular beam epitaxy on [100]-oriented GaAs substrates and characterized by x-ray diffraction.[5] Their parameters are listed in Table I. Beyond the period d and the average aluminum content $\bar{x}$, the x-ray diffraction studies provide a good determination of the layer thicknesses n_1 (GaAs) and n_2 ($Ga_{1-x}Al_xAs$) (number of monolayers) by refinement between experimental and calculated structure factors. The Raman scattering experiments have been performed in the backscattering configuration on the (100) face. Under these conditions, the transverse vibrations are never Raman active. In all samples but $S1$, we have observed at least two folded longitudinal acoustical (LA) lines and determined thereby values of the sample parameters which were always consistent with the x-ray determinations.

TABLE I. Sample parameters as defined in the text. For samples $S6$ and $S8$ the parameters have been estimated from the growth conditions.

	d (Å)	$\bar{x}$	n_1	n_2
$S1$	28	0.13	6	4
$S2$	29.2	0.123	6	4
$S3$	40.3	0.126	8	6
$S4$	39.1	0.137	8	6
$S5$	51	0.147	9	9
$S6$	· · ·	0.15	11	11
$S7$	54.4	0.141	12	7
$S8$	· · ·	0.15	14	14
$S9$	81.4	0.145	17	12

Figure 1 shows Raman spectra in the GaAs optical frequency range, obtained on some of the samples in the $z(x,y)\bar{z}$ configuration. In the same energy range, but in the

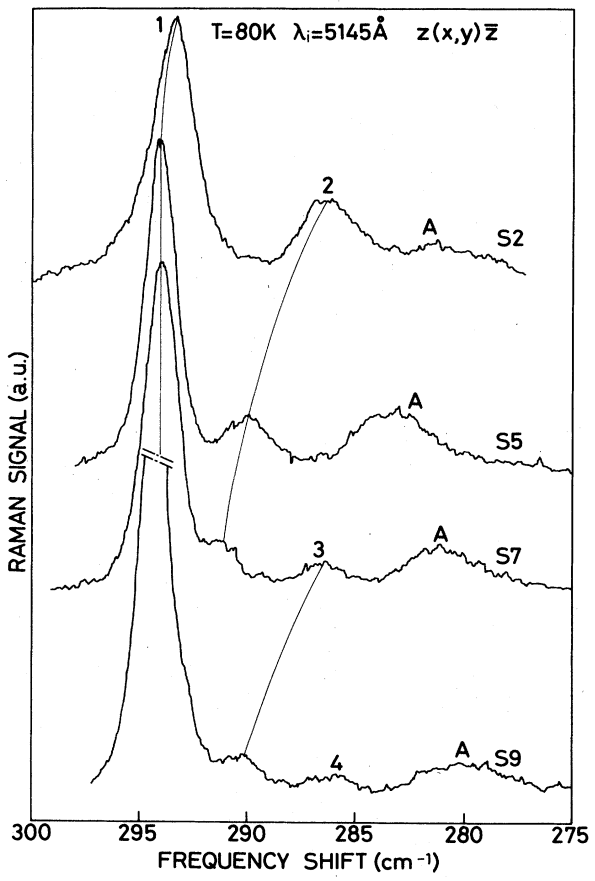

FIG. 1. Raman spectra in the optical frequency range. The line indexes are defined in the text and the spectrum indexes in Table I.

$z(x,x)\bar{z}$ configuration, we have observed a flat spectrum. Let us first recall that $Ga_{1-x}Al_xAs$ exhibits a two-mode behavior. For $x \simeq 0.3$, the GaAs-type LO frequency (ω_2) lies about 10 cm^{-1} below the one of GaAS (ω_1), whereas the less intense AlAs-type one lies 80 cm^{-1} above. We will no more consider the latter one. Regarding the superlattice as the stacking of two bulk materials, we would predict the emergence in the (ω_1, ω_2) energy range in the $z(x,y)\bar{z}$ configuration of one GaAs LO line and one less intense GaAs-type LO line of $Ga_{1-x}Al_xAs$. Our more complicated experimental results give evidence of the effect of confinement on the optical phonons. The frequency shift of line 1 is very close to the LO-frequency shift in GaAs but displays the same effect, but smaller, as do the shifts in lines 2 and 3 (see Fig. 1): it decreases as n_1 decreases. The frequency shift of line A essentially depends on the slightly varying aluminum contents in the $Ga_{1-x}Al_xAs$ layers.

To interpret these results, we will first recall some qualitative results from Ref. 4. In contradistinction with the acoustical frequency bands which almost coincide in GaAs and $Ga_{1-x}Al_xAs$, giving rise to propagative folded modes, the GaAs LO band and the GaAs-type LO band in $Ga_{1-x}Al_xAs$ are only partially overlapping. Between ω_1 and ω_2, the vibrations are localized in GaAs and display thereby no dispersion: the superlattice behaves like a phonon "multiquantum well." The phonon "quantum level" frequencies depend on the GaAs layer thickness and weakly on the well depth $\omega_1 - \omega_2$. We assign lines 1–4 to such optical-phonon quantum levels. Below ω_2, dispersive propagative vibrations appear. We assign line A to the higher energy one.

In order to analyze more quantitatively our experimental results, we used a Kronig-Penney-type model of the dispersion curves along the superlattice axis. We describe the LO vibrations in both materials AB and AC by a linear chain model. The eigenmodes of the superlattice are taken, in each layer, as a linear combination of a backward and a forward propagating eigenmodes of the related bulk material. As it actually holds for GaAs and $Ga_{1-x}Al_xAs$, we assume the common atom A to be the heaviest one. As well, the force constant K and the lattice parameter a are taken equal in both materials. Writing the superperiodicity and the hereinafter described boundary conditions, we obtain the optical-phonon dispersion curves and eigendisplacements. The interface being located on an A atom, we express the continuity of the eigenmodes at the interface by identifying the displacement of the interface atom A with the ones it would have, if embedded in AB or in AC. The dispersion curves are then the solutions of

$$\cos(qd) = \cos(n_1k_1a)\cos(n_2k_2a) - \alpha\sin(n_1k_1a)\sin(n_2k_2a) \ ,$$

with

$$\alpha = \frac{1-\cos(k_1a)\cos(k_2a)}{\sin(k_1a)\sin(k_2a)} \ ,$$

k_i being the wave vector, eventually complex, at frequency ω, in medium i. To evaluate the Raman activities R_{xx} [$z(x,x)\bar{z}$ configuration] and R_{xy} [$z(x,y)\bar{z}$], we use the same method as in Ref. 6. We do not fit the values of the polarizabilities α_{xx} and α_{xy} in each material and rather use equal values for α_{xy} (and α_{xx}) in both materials, which is a good approximation. As an illustration, we present in Figs. 2 and 3 some results on a typical superlattice consisting of

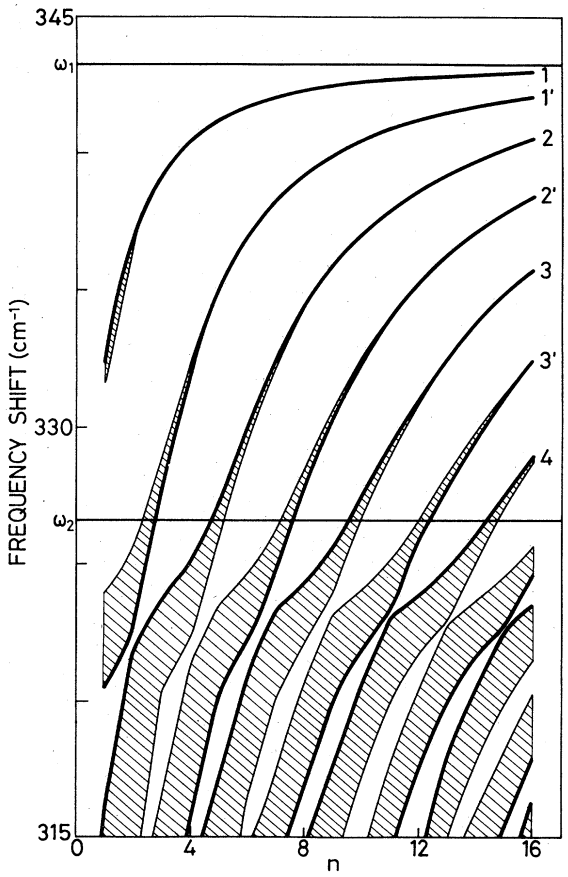

FIG. 2. Frequency shifts of the zone-center (thick line) and zone-boundary (thin line) eigenmodes as a function of the well width n. The hatched regions contain the allowed energies. The sample is described in the text as well as ω_1, ω_2 and the labels.

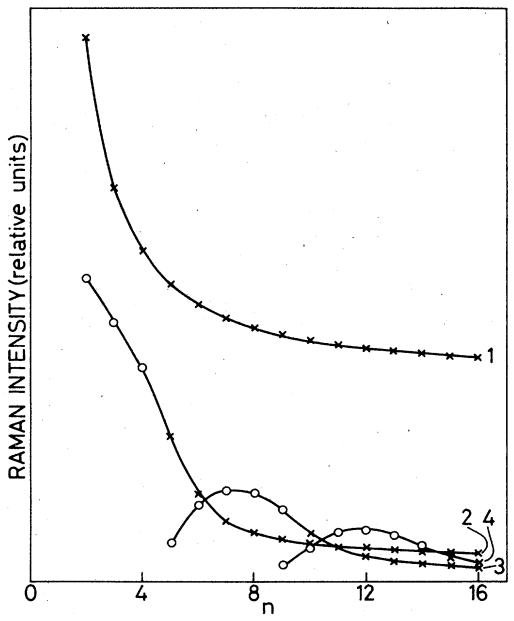

FIG. 3. Raman activity R_{xy} as a function of the well width n for four eigenmodes already labeled in Fig. 2. The calculated values are represented by crosses (circles) if the related mode is in the well (above the barrier).

alternating n unit cells of medium 1 (masses $M_1=70$ amu, $m_1=40$ amu) and 5 unit cells of medium 2 ($M_2=M_1$, $m_2=47$ amu). We have chosen $K=1.5\times10^6$ cm^{-2}amu, a typical value for III-V compounds. Medium 1 acts as a phonon well and medium 2 as a phonon barrier. The barrier height is equal to 16.7 cm^{-1}. Figure 2 shows the allowed energy bands as a function of the well width n. In the well, the phonon levels are almost undispersive and their frequency shifts decrease as the well width decreases. Their zone-center components display alternating B_2 (modes $1,2,\ldots$) and A_1 ($1',2',\ldots$) symmetry of the D_{2d} point group. As they reach the top of the well (ω_2), they continuously transform in dispersive energy bands. In Fig. 3 we show the variation of the Raman tensor R_{xy} (calculated per unit cell) as a function of the well width for the four first B_2 modes. R_{xx} is zero because of symmetry, as R_{xy} is for A_1 modes. The value of R_{xx} for A_1 modes vanishes only if we take α_{xx} equal in both materials, but stays always small. This explains the absence of Raman signal, due to the A_1 modes, in the $z(x,x)\bar{z}$ configuration. Let us come back to the B_2 modes: the higher energy mode 1 is always well localized in the well and R_{xy} is large owing mainly to the contribution of the well atoms. Concerning the other modes ($2,3,\ldots$) their localization in the well becomes weak as they approach the top of the well (ω_2). Their Raman activity R_{xy} then increases and the contribution of the barrier atoms is already dominant before the modes merge in the propagation energy range. A further decrease of n gives rise to a decrease both in frequency and Raman activity of the now propagative modes. In conclusion, if we except mode 1 which is clearly associated with well vibrations, all other modes display complicated behaviors: particularly, it is difficult to define any barrier related vibration.

To fit the experimental results, we have benefited from the following property of the Kroning-Penney dispersion relation: the dispersion properties of both bulk materials only appear through the expressions of $\cos(k_1a)$ and $\cos(k_2a)$ as a function of ω. We have, therefore, used the experimentally determined dispersion curve[7] of the LO phonon of GaAs in the (100) direction through a fairly good fitted expression:

$$\cos(ka)=1+\frac{\omega^2}{B}[\omega^2-\omega^2(k=0)]\ ,$$

where B depends on the curvature of the branch. For the GaAs-type mode of $Ga_{1-x}Al_xAs$, we have checked the small influence of its curvature on the phonon quantum-level frequencies and taken the same value as in GaAs. The resulting frequencies strongly depend on the well width, slightly on the barrier height, and unsignificantly on the barrier width. We have obtained a good fit of experimental results using the constant value of 294.6 cm^{-1} for the GaAs LO frequency. The zone-center GaAs-type LO frequency in $Ga_{1-x}Al_xAs$ has been fitted for each sample, taking into account the compositional variations. The quality of the fit can be appreciated on Fig. 4 where the experimental results are represented as a function of the GaAs layer width and compared with two calculations using two extreme values of ω_2: 280 and 286 cm^{-1}. The experimental points should lie between the curves. The fit is rather good despite a slight tendency of the model to overestimate the confinement. Concerning the Raman intensity, our phenomenological approach does not provide the eigenmodes and, therefore, the Raman intensities. We only perform a qualitative comparison with the calculations shown in Fig. 3. We obtain a good description of the spectra ($S1,S2$ similar to $n=5$; $S3,S4,n=8$;$S7,S8,n=11$).

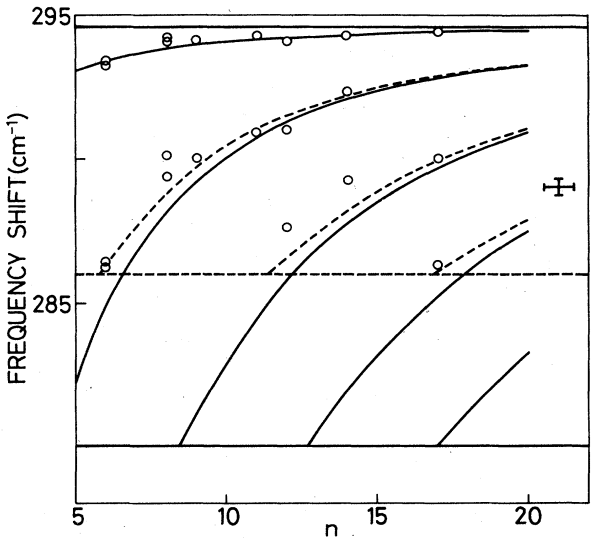

FIG. 4. Experimental frequency shifts (circles) compared with two calculations: solid line: $\omega_2=280$ cm^{-1}; dashed line: $\omega_2=286$ cm^{-1} (see the text).

In summary, we have observed and analyzed the emergence of new Raman lines in the GaAs/$Ga_{1-x}Al_xAs$ superlattice, assigned to LO-phonon quantum levels.

Laboratoire de Bagneux, Division PMM, is Laboratoire Associé au CNRS (LA 250).

[1]C. Colvard, R. Merlin, M. V. Klein, and A. C. Gossard, Phys. Rev. Lett. **45**, 298 (1980).
[2]J. Sapriel *et al.*, Phys. Rev. B **28**, 2007 (1983).
[3]B. Jusserand, D. Paquet, A. Regreny, and J. Kervarec, Solid State Commun. **48**, 499 (1983).
[4]B. Jusserand, D. Paquet, A. Regreny, and J. Kervarec, J. Phys. (Paris) Colloq. **45**, C5-145 (1984).
[5]J. Kervarec *et al.*, J. Appl. Cryst. **17**, 196 (1984).
[6]A. S. Barker, Jr., J. L. Merz, and A. C. Gossard, Phys. Rev. B **17**, 3181 (1978).
[7]J. L. T. Waugh and G. Dolling, Phys. Rev. **132**, 2410 (1963).